Indian Journal of Fibre & Textile Research
Vol. 47, September 2022, pp. 275-280
DOI: 10.56042/ijftr.v47i3.48452

Production and characterization of polyurethane ultrafine fibre webs containing boric acid by electrospinning

Ayben Pakolpakçıl [a] & Zbigniew Draczyński

Institute of Materials Science of Textiles and Polymer Composites, Lodz University of Technology, 116 Żeromskiego Street 90 – 924 Lodz, Poland

Received 4 April 2021; revised received and accepted 12 January 2022

A novel material has been developed by electrospinning of thermoplastic polyurethane (TPU) ultrafine fibre webs containing boric acid (BA). The chemical characterization of the TPU/BA fibrous webs is determined by the energy dispersive spectrometer and the Fourier transform infrared spectroscopy. The morphologies and thermal properties of the webs obtained are investigated by scanning electron microscopy and the differential scanning calorimeter respectively. The electrospun fibrous webs' air permeability performance and thickness are also measured. The morphologies of TPU fibrous webs change slightly by adding BA, and the fibre structures are maintained. The results obtained demonstrate that the electrospun TPU/BA fibrous webs may have a wide variety of potential applications in protective textiles and high-performance filters.

Keywords: Boric acid, Electrospinning, High performance filter, Polyurethane, Permeability, Ultrafine fibre webs

1 Introduction

In the previous two decades, electrospinning has become the preferred method for creating micro-nano scale polymeric fibre, which is in high demand due to the requirement of cheap raw materials and the effectiveness of fabrication technology for mass production of these products. According to the Grand View Research Inc. report, the global nanofibres market size was estimated as USD 477.7 million in 2016. In addition, it is predicted that changes in customer and product trends will drive the market. It is expected that the manufacture of a wide range of products from composite nanoscale fibres will drive industry innovation and thus increase its penetration in the automotive and textile markets[1].

Nanofibres have unique characteristics, such as high specific surface and small pore sizes, and offer a wide range of applications, including textiles, food, energy, and environment. Electrospinning is a simple, versatile, and cost-effective technique to produce ultrafine polymer fibres. During the electrospinning process, the polymer solution is extruded from the capillary tube by electrical field force and a Taylor cone can be formed at the capillary tip. Positive charges will accumulate on the surface of the Taylor cone as the electrical field intensity increase, which overcomes surface tension and induces fluid ejection. The fluid injected may be extended several times longer than the original length as the spinning phase continues. The solvent evaporates quickly, and a continuous ultrafine polymer fibre is produced[2-4]. As a result, electrospun nanofibres have gained a great deal of interest due to the ease of manufacture of multifunctional nanofibrous materials for use in many applications such as, textile, food packing, battery, and water purification systems[3,4].

Boric acid (H_3BO) is a weak acidic and water-soluble mineral. It is a white powder containing boron and water. It is not flammable, explosive or combustible. It has antibiotic properties against both fungal and bacterial infections. Previous studies have shown that boron is a bioactive mineral element. It has many nutritional benefits for higher animals and humans. Boric acid has low toxicity, easy availability, and low cost, making it an alternative candidate for the development of functional materials[5-7]. Some researchers have drawn attention to these characteristics, and its applicability for textile materials has been investigated. Uslu *et al.*[8] investigated the production of nylon 6 doped with boron nanofibres by electrospinning. Uslu *et al.*[9] also reported that boron-

[a]Corresponding author.
E-mail: ayben_p@yahoo.com; ayben.pakolpakcil@nisantasi.edu.tr

Present address: Textile and Fashion Design Department, Nişantaşı University, Maslak Mahallesi, Taşyoncası Sokak, No: 1V ve No:1Y Sarıyer-İstanbul, Türkiye.

doped poly(vinyl) alcohol (PVA)/HfO_2 nanofibres had been produced by electrospinning. Selvakumar *et al.*[10] investigated the flammability properties of electrospun polyamide/boric acid nanocomposite fibres. Isık *et al.*[11] reported PVA electrospun nanofibres; boric acid complexes of these nanofibres were manufactured by electrospinning, and their antibacterial properties were explored. Parin *et al.*[12] developed a polyamide 6/honey/boric acid nanofibrous mats by electrospinning for wound dressing applications. Polyurethane (PU) is an important polymer, widely used in various fields, such as automotive, furniture, construction, clothing, and footwear. PU is widely used for its low cost, chemical resistance, tear resistance, abrasive resistance, and high load-bearing[13,14]. Electrospun polyurethane textiles have been used as air filters[15], scaffolding[16], wound dressings[17], protective clothing[18], packaging[19], water filters[20], wearable sensors[21], and vascular grafts[22]. To date, no study has been conducted to investigate the effect of BA on electrospun PU webs.

This study examines the electrospinning of thermoplastic polyurethane (TPU) fibrous webs including boric acid and investigates the effects of boric acid on the resulting webs properties. The modified TPU fibrous webs are characterized in terms of their morphology, chemical composition, thermal properties, air permeability performance, and thickness. This study will also expand the applications of boric acid, an abundantly available mineral product.

2 Materials and Methods

2.1 Materials

TPU polymer, a commercial product (Elastollan® is a polyester-based polyurethane), was obtained from BASF. The boric acid (BA) was obtained from Chempur, and N, N dimethylformamide (DMF 98%), supplied by Sigma-Aldrich, was used as a solvent for the polymer.

2.2 Methods

TPU polymer was dissolved in DMF by mixing in a magnetic stirrer for 24 h with a concentration of 13% (w/v). After that, BA was added separately to the prepared TPU polymer solution in two different concentrations (2% and 3 wt. %). The mixtures were then stirred for 2 h.

Electrospinning was performed using a home-made electrospinning machine with a horizontal setup. The electrospinning solutions was placed into a plastic syringe (20 mL) with a metal capillary having an inner diameter of 0.60 mm. The electrospinning process was performed at an applied voltage of 25 kV, a flow rate of 1 mL/h, a collector distance tip of 20 cm and a drum speed of 180 rpm. The fibrous webs were collected on aluminium foil. Approximately 15 mL of polymer solutions was collected until the samples had reached a certain thickness. All solution preparations and electrospinning processes were carried out at room conditions.

2.3 Measurement and Characterization

The viscosity of the TPU and TPU/BA solutions was measured with a rheometer (Anton Pear rheolab QL) at a constant speed of 100 rpm at 25 ℃. Three measurements were performed. The mean and standard deviation values of the viscosity were calculated.

The morphology and elemental compositions of the electrospun TPU and TPU/BA fibrous webs were examined using scanning electron microscopy (SEM) and an energy dispersive spectrometer (EDS) (FEI Nova NanoSEM 230). The average diameter, their standard deviations, and diameter distribution of the fibres in the webs were calculated by using the Image J Tool for at least 100 measurements per sample.

The chemical structures and functional groups of the electrospun TPU and TPU/BA fibrous webs were characterized via a Fourier transform infrared (FTIR) spectroscopy (Nicolet 6700, Thermo Scientific), operating in the range of 600-4000 cm^{-1}.

The thermal behaviour of the electrospun TPU and TPU/BA fibrous webs was investigated using a differential scanning calorimeter (DSC Q2000, TA Instruments). The fibrous webs were weighed and sealed in aluminium pans. Then, the temperature was raised from -50°C to 210°C under a nitrogen flow of 50 mL/min at a heating rate of 20°C/min.

The air permeability properties of the electrospun TPU and TPU/BA fibrous webs were examined using a Textest FX 3300 air permeability tester. The tests were conducted according to ISO 9237 standard; following sealing, a sample with a test area of 20 cm^2 was subjected to a pressure of 100 Pa. Five measurements for each sample were recorded and a mean value was calculated. The thickness of the fibrous webs was measured by a digital micrometre with a 0.001 mm accuracy at ten points, and the average thickness was calculated from these measurements

3 Results and Discussion

3.1 Morphological Characterizations of Electrospun Webs

SEM was used to investigate the surface morphology, shape, and size of TPU and TPU/BA

fibrous webs. The SEM images with different BA concentrations (2 and 3 wt %) are shown in Fig. 1. The electrospun TPU has a continuous and uniform structure [Fig. 1(a)]. In the previous study[23], the electrospun TPU membrane had a diameter of 200-500 nm. In this study, the average diameter of the electrospun TPU ultrafine fibres is 387 nm and this result agrees with the literature[23].

According to the SEM images of TPU containing BA nanofibres, the structures were wavy and less regular on the surface of fibres [Figs 1(b) and (c)]. SEM images show that the addition of BA to the TPU

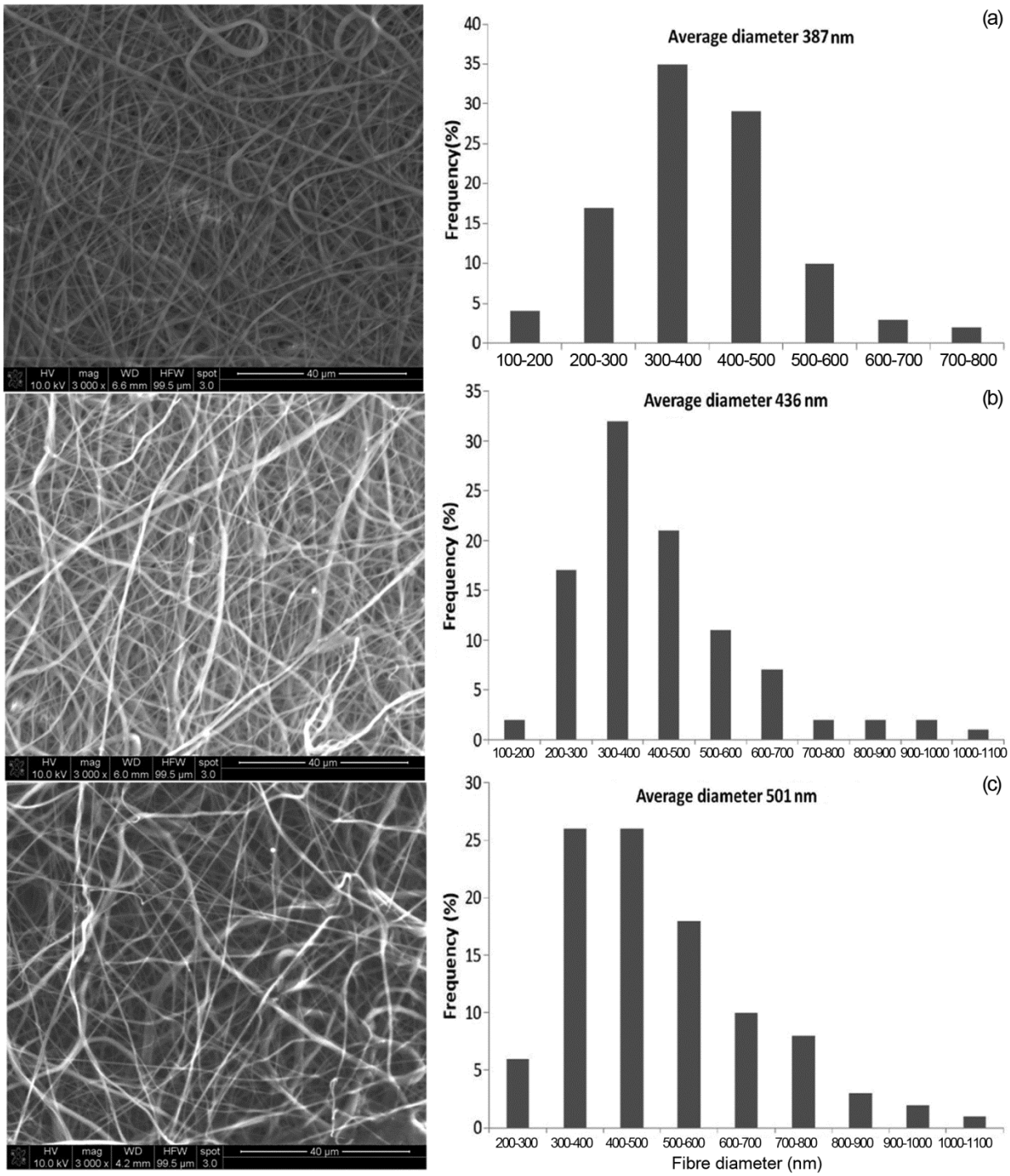

Fig. 1 — SEM morphology and diameter distribution of electrospun TPU and TPU/BA webs with BA content (a) TPU, (b) TPU/2BA, and (c) TPU/3BA (×3000)

Table 1 — Viscosity of electrospinning solutions

Electrospinning solutions	Viscosity, Pa.s
TPU	0.3961 ± 0.004
TPU/2BA	0.4221 ± 0.002
TPU/3BA	0.4377 ± 0.002

polymer solution causes an increase in the fibre diameter from 387 nm to 436-501 nm. This can be explained by increasing viscosity. The electrospinning process and the morphology of fibres are influenced by the viscosity of the solution[3,4]. This is determined before electrospinning. The TPU and TPU/BA viscosity values are shown in Table 1. The viscosity of TPU shows the lowest viscosity value of 0.3961 Pa.s, which is increased to 0.4221 and 0.4377 Pa.s by the addition of 2 wt % and 3 wt % BA respectively. The increment in electrospinning solutions' viscosity may be attributed to interactions between polyurethane and boric acid with hydrogen bonding. The viscosity of the solution creates a force opposite to the electrostatic repulsion that is responsible for the stretching and thinning of the solution jet. Previous studies have shown that higher viscosity results in larger fibre diameters[3,4]. It is expected that the viscosity would increase as the amount of BA concentration is increased. The increase in viscosity of the electrospinning solutions results in a large amount of polymer at the end of the jet, resulting in a larger nanofibre diameter. Uslu *et al.*[8] indicated that mixing boron compounds with PVA polymer solution increases the viscosity of the solution.

To investigate the effect of BA on TPU polymer solution for electrospinning, different concentrations of BA (2 and 3 wt. %), were fabricated. SEM images showed that the average diameter of nanofibres increased with the addition of BA. Generally, the size distributions of the fibres [Figs 1(a) – (c)] were collected between 300 and 500 nm. The morphologies of the electrospun TPU and TPU fibrous webs containing different quantities of BA indicated randomly oriented fibres with similar diameters along their lengths in the strip as well as no bead-like structure.

3.2 EDS Analysis of Electrospun Webs

The EDS analysis has been performed to check the insightful understanding that the added BA is present on electrospun fibrous webs. The results of the electrospun TPU and TPU/BA fibrous webs EDS analysis are presented in Fig. 2. The composition of the electrospun TPU web consists of almost 70 wt % of C and, 30 wt of % O, while the composition of the

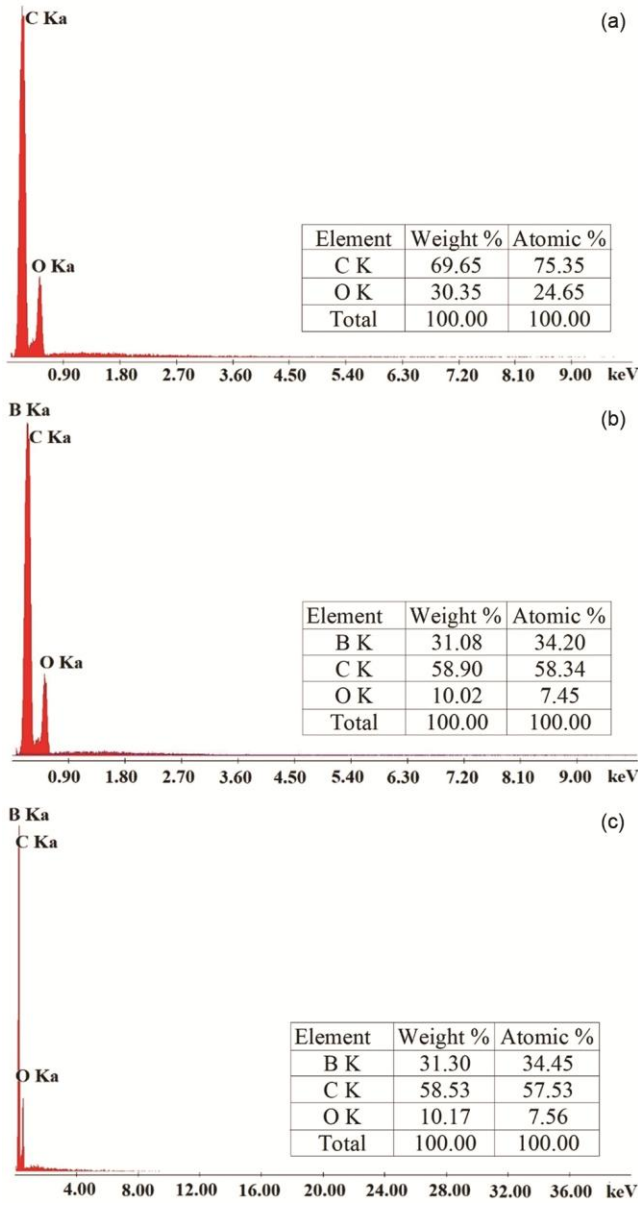

Fig. 2 — EDS images and elemental results of electrospun webs (a) TPU, (b) TPU/2BA, and (c) TPU/3BA

electrospun TPU/BA webs consists of almost 31 % of B, 59 % of C and, 10 wt % of O. The EDS spectra show a peak of B for the electrospun webs, confirming the presence of BA in the chemical composition present over the ultrafine fibres.

3.3 FTIR Spectra

The functional groups of BA, TPU, and TPU/BA webs are determined by FTIR (Fig. 3). The characteristic peaks of the TPU observed at 3197^{-1}, 2954 cm^{-1}, 1726 cm^{-1}, 1526 cm^{-1}, 1219 cm^{-1}, 1067 cm^{-1}, and 768 cm^{-1} are assigned to (N-H), (C-H), (C=O), (C=C), (C-C), (C-O), and (C-H) on substituted

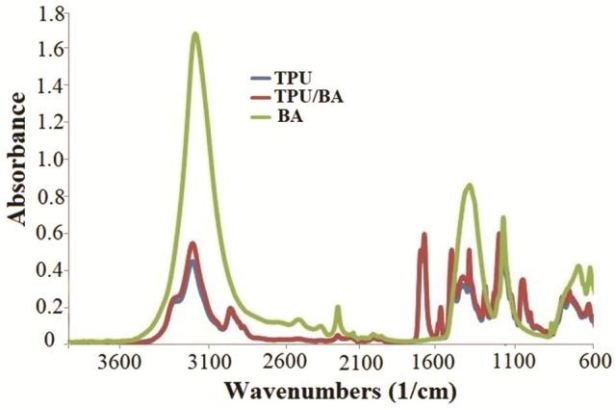

Fig. 3 — FTIR spectra of BA, electrospun TPU, and TPU/BA webs

benzene respectively. The peaks are in agreement with the TPU reports available in the literature[14, 17, 22]. The structure of the BA is characterized by typical absorption bands at 3181 cm^{-1}, 1409 cm^{-1}, and 1193 cm^{-1}, which represent (O-H), (B-O) and (B-OH) respectively. The outcome is consistent with the literature[24]. The characteristic peaks of the TPU/BA composite nanofibre observed at 3198 cm^{-1}, 2954 cm^{-1}, 1732 cm^{-1}, 1526 cm^{-1}, 1413 cm^{-1} and 1190 cm^{-1} are assigned to (O-H), (C-H), (C=O), (C=C), (B-O) and (B-OH) respectively. Most of the peaks of TPU and BA overlap in the TPU/BA composite nanofibres, because of their similarity and shifting. Peak intensities are found to be lower with TPU content as compared to pristine BA. TPU and BA are prone to form many inter-hydrogen bonds. However, when the electrospun TPU fibrous webs and BA containing TPU webs are examined, the increase in peak intensity is evidence of the presence of BA in the ultrafine fibres. This finding shows that boric acid is successfully integrated into the TPU fibres.

3.4 Thermal Properties of Electrospun Webs

The thermal properties of the electrospun fibrous webs are examined by a differential scanning calorimeter. The DSC thermograms of the electrospun TPU and TPU/BA webs are presented in Fig. 4. No significant change is observed at the glass transition temperature (T_g), as indicated in the manufacture at around -40°C (ref. 25). The electrospun TPU webs exhibit two endothermic peaks, attributed to two melting temperatures (T_m) at 141°C and 201°C respectively. Xu *et al.*[26] has shown that these two endotherms are due to the melting of the ordered structure in the hard phase and the microphase of the

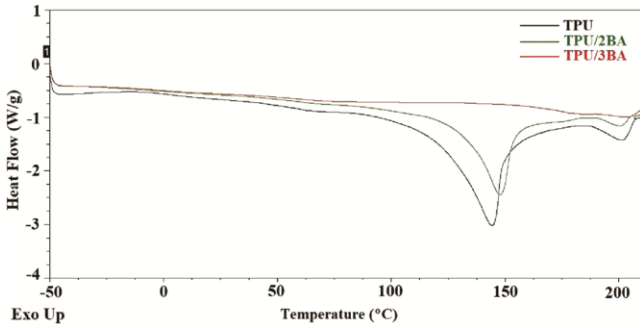

Fig. 4 — DSC thermograms of electrospun TPU and TPU/BA webs

Table 2 — Some properties of the electrospun webs (average ± standard deviation)

Electrospun webs	Thickness µm	Air permeability $cm^3/cm^2.s$	Average fibre diameter, nm
TPU	126 ± 18.2	0.62 ± 0.01	387 ± 120
TPU/2BA	117 ± 13.6	0.44 ± 0.04	436 ± 190
TPU/3BA	134 ± 32.4	0.43 ± 0.05	501 ± 168

soft and hard segments. The electrospun TPU/2BA webs exhibit two endothermic peaks, attributed to two melting temperatures at around 143°C and 200°C. This increase in the $T_{m(soft)}$ could be attributed to the effects produced by the boric acid in the soft segment domains, leading to the increase in degree of crystallinity. This increment in $T_{m(soft)}$ could be linked to the actions of boric acid on the soft segment domains, which result in an increase in crystallinity. The electrospun TPU/3BA webs exhibit an endothermic peak, attributed to the melting temperature at 204°C. As can be seen from Fig. 4, higher concentrations of BA are influenced by TPU/BA fibres. This result is attributed to the presence of BA in the webs, which influences the orientation of the molecular chains.

3.5 Air Permeability of Electrospun Webs

Air permeability is a significant performance parameter for textiles and membranes. Many parameters may affect the air permeability of materials, such as fibre diameter, thickness, and porosity[27,28]. The results of the air permeability test are given in Table 2. The air permeability values of the electrospun TPU, TPU/2BA, and TPU/3BA webs are 0.62, 0.44, and 0.43 $cm^3/cm^2.s$ respectively. The air permeability values indicate that the addition of BA to the electrospun TPU fibrous webs causes a decrease. The explanation may be that, the irregular surface [Figs 1(b) and (c)] of the fibre provides more resistance to air flow. The similar value is observed by Liu *et al.*[29], who

reported that the air permeability of the electrospun PAN mat (354 nm) is measured at 0.55 cm^3/cm^2.s. As a result, the TPU and TPU/BA fibrous webs can be accessible to the passage of air. Nanofibres have highly compact and dense structures, and hence the air flow is low. It is a supporting tool with low air permeability in materials, depending on their area of use, such as air filters or breathing masks.

4 Conclusion

This work aims to approach the use of boric acid for the production of ultrafine fibre webs by electrospinning technique using a non-expensive and simple methodology. The study shows the process and characterization of the electrospun BA containing TPU fibrous webs. SEM images of the electrospun fibrous webs show that TPU/BA webs has higher fibre diameters as compared to pure TPU webs. Fibre diameter increases as BA content is increased. The EDS analysis demonstrates the incorporation of BA into the TPU fibrous webs. The melting temperature of the polymers used in fibrous membranes is observed to be affected by the presence of BA. Overall, due to the high specific surface and small pore sizes, electrospun TPU/BA fibrous webs could be promising functional textile materials, such as filters, protective clothes and antibacterial textiles. The findings of this research will likely open new directions for future studies of the electrospun TPU/BA webs for many other applications.

References

1 Nanofibers Market Size, Share & Trends Analysis Report 2017-2024, (Grand View Research Inc.), https://www.grandviewresearch.com/industry-analysis/nanofibers-market (accessed on 1.03.2021).

2 Pakolpakçıl A & Draczynski Z, *J Text Inst*, 113 (2021) 1908.

3 Islam M S, Ang B C, Andriyana A & Afifi A M, *SN Appl Sci*, 1 (2019) 1248.

4 Thenmozhi S, Dharmaraj N, Kadirvelu K & Kim H Y, *Mater Sci Eng B*, 217 (2017) 36.

5 Forrest H N & Susan L M, *Evid-Based Compl Alt*, 16 (2011) 3.

6 Abdelnour S A, Abd El-Hack M E, Swelum A A, Perillo A & Losacco C, *J Trace Elem Med Biol*, 50 (2018) 296.

7 Nielsen F H, *J Trace Elem Med Biol*, 28 (2014) 379.

8 Uslu I, Çelikkan H, Atakol O & Aksu M L, *Hacet J Biol Chem*, 36 (2008) 2.

9 Uslu I, Altas A, Aksu M L & Gökmeşe F, *Hacet J Biol Chem*, 37 (2009) 1.

10 Selvakumar N, Azhagurajan A, Natarajan T S & Khadir M M A, *J Appl Polym Sci*, 126 (2012) 614.

11 Isik A F, Keskin N O S & Ulcay Y, *J Text Inst*, 110 (2019) 4.

12 Parin F N, Terzioğlu P, Parin U, Yeşilyurt A, Eroğlu M & Yildirim K, *Mater Today Commun*, 29 (2021) 102921.

13 Akduman C & Kumbasar E P A, in *Electrospun Polyurethane Nanofibers*, edited by F Yilmaz (IntechOpen), 2017.

14 Pakolpakçıl A & Draczynski Z, *Materials*, 14 (2021) 6949.

15 Mohraz M H, Golbabaei F, Yu I J, Mansournia M A, Zadeh A S & Dehghan S F, *Int J Environ Sci Technol*, 16 (2019) 681.

16 Letha S S, Kumar A S, Nisha U & Rosemary M J, *J Text Ins.* 113 (2022) 378.

17 Mistry P, Chhabra R, Muke S, Narvekar A, Sathaye S, Jain R & Dandekar P, *Mat Sci Eng C*, 119 (2021) 111316.

18 Kim Y N, Ha Y M, Park J E, Kim Y O, Jo J Y, Han H, Lee D C, Kim J & Jung Y C, *Polym Test*, 93 (2021) 107006.

19 Mrunalini K G, Pudke S P & Sharma C S, *J Appl Polym Sci*, 138 (2021) 11.

20 Tijing L D, Ruelo M T G, Amarjargal A, Pant H R, Park C H, Kim D W & Kim C S, *Chem Eng J*, 197 (2012) 41.

21 Wang Y, Li W, Zhou Y, Jiang L, Ma J, Chen S, Jerrams S & Zhou F, *J Mater Sci*, 55 (2020) 12592-12606.

22 Gostev A A, Shundrina I K, Pastukhov V I, Shutov A V, Chernonosova V S, Karpenko A A & Laktionov P P, *Polymers*, 12 (2020) 845.

23 Nirmala R, Nam K T, Navamathavan R, Park S J & Kim H Y, *Nanoscale Res Lett*, 6 (2011) 2.

24 Shawgi N, Li S X & Wang S, *Ceram Int*, 43 (2017) 13.

25 Basf, Elastollan® technical data sheet, http://www.automchina.com/Basf%20C95A.pdf (accessed on 1.03.2021).

26 Xu J, Cheng L, Zhang Z, Zhang L, Xiong C, Weishan H, Xieb Y & Yang L, *RSC Adv*, 9 (2019) 818.

27 Liu Y Q, Feng J W, Zhang C C, Teng Y, Liu Z & He J H, *Therm Sci*, 22 (2018) 4.

28 Pakolpakçıl A, Draczyński Z, Szulc J, Stawski D, Tarzyńska N, Bednarowicz A, Sikorski D, Hernandez C, Sztajnowski S, Krucińska I & Gutarowska B, *Appl Sci*, 11 (2021) 8219.

29 Liu X, Lin T, Fang J, Yao G, Zhao H, Dodson M & Wang X, *J Biomed Mater Res A*, 94 (2010) 2.